

EFFECT OF DEFECTS ON FATIGUE TESTS OF AS-BUILT Ti-6Al-4V PARTS FABRICATED BY SELECTIVE LASER MELTING

Haijun Gong*, Khalid Rafi*, Thomas Starr†, Brent Stucker*

*Department of Industrial Engineering, †Department of Chemical Engineering,
J. B. Speed School of Engineering, University of Louisville, Louisville, KY 40292

REVIEWED, Accepted August 16, 2012

Abstract

Defects can be found in parts made using Selective Laser Melting (SLM) due to balling effects and other types of localized irregularities. This study investigates how defects affect the fatigue performance of Ti-6Al-4V samples in an SLM as-built surface finish condition. Fatigue samples were built and heat treated for stress relief. In order to investigate the effect of defects, a series of fatigue samples were designed with built-in cylindrical and double-conical defects. Tests were carried out to correlate maximum stress to the number of cycles to failure. Optical and scanning electron micrographs were utilized to compare and analyze crack initiation and propagation characteristics. Based on the results, the influence of defects on fatigue properties is discussed.

Introduction

Additive Manufacturing (AM) refers to the process of joining materials to make objects from three-dimensional Computer Aided Design data, usually layer upon layer, as opposed to subtractive manufacturing methodologies, such as traditional machining [1]. It significantly simplifies the process of producing complex 3D objects directly from CAD data without process planning. The operator only needs some basic dimensional details and a small amount of understanding as to how the AM machine works and the materials that are used [2]. Application of additive manufacturing technology to fabricate complex three-dimensional components is one promising direction in industrial and medical field [3, 4]. This approach is rapidly changing the pattern of designers and processors for creating objects with desired shape and structure. Many additive manufacturing methods have been applied in many variations to satisfy industrial and medical needs for rapidity and flexibility.

Titanium alloys such as Ti-6Al-V4 are widely adopted in aerospace, biomedical and industrial fields due to its inherent properties of fracture resistance, fatigue behavior, corrosion resistance and biocompatibility [5]. In recent years, selective laser melting (a metal powder bed fusion AM process which utilizes a laser to melt metal powder layer-by-layer.) has shown great versatility for fabricating parts from numerous types of metallic powders such as stainless steel, maraging steel, cobalt chromium and Ti-6Al-4V. Titanium alloys are extensively investigated and utilized in SLM processes. Thus, there is interest in quality attributes of SLM Ti-6Al-V4 components as compared to wrought or cast plus post heat treatment-produced components [6-8]. In order to give more insights to designers who are employing this technology, quality and life span of AM components must be carefully investigated, especially for metallic parts with defects. Thus, this research focuses on understanding how defects affect the fatigue life of as-built Ti-6Al-4V specimens fabricated using SLM. The stress-life plot is discussed based on the crack pattern of

the fracture surfaces. Fractography of each crack pattern is shown for interpreting the crack initiation and propagation process.

Material and Experimental Plan

Ti-6Al-4V powder

The material used for this investigation is EOS Ti64, which fulfills requirements of ASTM F1472 (for Ti-6Al-4V) regarding maximum concentration of impurities [9]. Fig.1 shows the powder morphology under a scanning electron microscope. The powder was measured using a Microtrac S3000 laser-based particle size analyzer. Its particles have a size distribution between 25 μm (D_{10}) and 53 μm (D_{90}). The particle size is nearly normally distributed with Mean Volume Diameter around 38 μm .

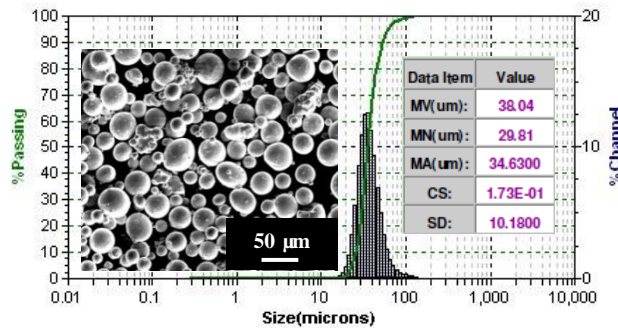


Fig. 1 EOS Ti-6Al-4V powder morphology and particle size distribution

Fatigue testing

Fatigue specimens were built vertically along their axis with an as-built gauge surface in an EOS M270 Direct Metal Laser Sintering (DMLS) system. The processing parameters from EOS are given in Table 1. Laser scanning along paralleled paths produced solidified layer. Contour scan was followed for each layer. It is believed that the specimen's density is almost 100% of STA Ti64 material [7]. Specimens conform to the ASTM E466 standard with a continuous diameter between ends. Some specimens were designed with cylindrical or double-conical (D-conical) internal defect by leaving a void in the CAD file, as shown in Fig. 2.

Table 1 Process parameters for fabricating Ti-6Al-4V fatigue specimens.

Laser power (W)	Scan speed (mm/s)	Hatch spacing (μm)	Layer thickness (μm)
170	1250	100	30

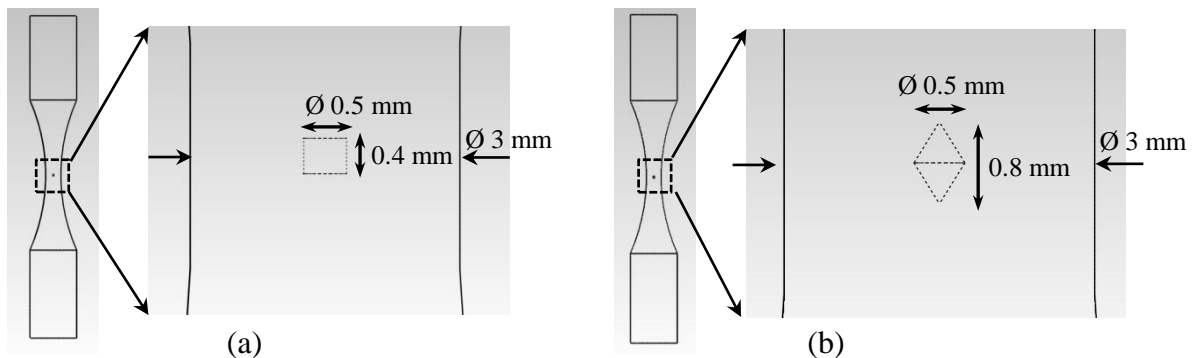


Fig. 2 CAD model of fatigue specimen (a) with cylindrical defect, (b) with D-conical defect

All specimens were heat treated at 650 Celsius for 4 hours in an argon filled furnace for stress relief and cooled down in the furnace to the room temperature. Light sand blasting was used to clean adhered particles from the surface of the specimens. Fatigue tests were conducted on an Instron ElectroPuls E10000 All-Electric Test Instrument. The specimens were tested using a continuous sinusoidal load with frequency 50 Hz. Stress ratio R (min/max stress amplitudes) is 0.1. The fracture surfaces were then examined by optical microscopy (Olympus MX51 industrial inspection microscope) and scanning electron microscopy (FEI Nova NanoSEM 600) for analyzing the effect of defect on the result of fatigue tests.

Results and Discussion

Characteristics of Fatigue Specimens

An as-built Ti-6Al-4V fatigue specimen is shown in Fig. 2. Through the scanning electron micrograph, it can be seen that the gauge surface is rough and irregular. Adhered particles were removed from the surface of the specimens by sand blasting. But some partially melted particles may be welded to the surface, resulting in convex surfaces which seem like speckles after blasting. But, in general, sand blasting does not affect the feature of as-built surface.

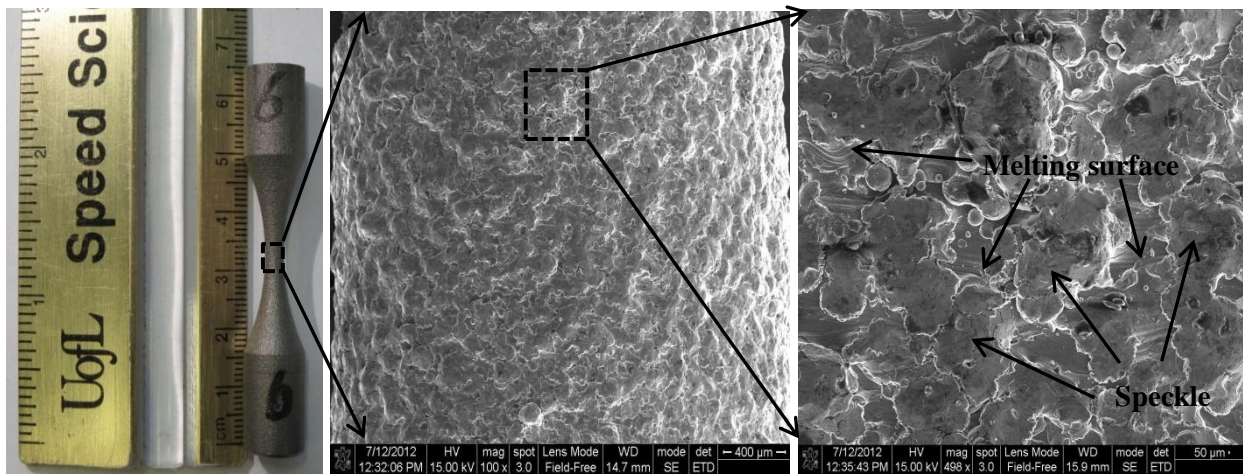


Fig. 3 As-built Ti-6Al-4V fatigue specimen and its surface feature

Fatigue results

High cycle fatigue tests can cause cracking in fatigue specimens. Stress-life plots of the fatigue specimens are shown in Fig. 4. The stress life of fatigue specimens without designed defects was rather low at a stress level higher than 500 MPa. Three specimens were tested at 500 MPa. One of them failed very quickly, while another two did not fail at all. When the stress level was lowered to less than 500 MPa, even at 10 million stress cycles the specimens did not fail.

It was assumed that the fatigue specimens would have lower stress life if a cylindrical or double-conical defect is included. Therefore, all the specimens with internal defects were tested with a maximum stress no larger than 500 MPa in order to investigate how fatigue life is affected. The results show that the fatigue life at some specific stress level is repeatable, such as fatigue specimens with a cylindrical or double-conical defect at 450 MPa. But, at other stress levels, the fatigue life could be distributed across a range. For example, the fatigue life at a 500 MPa stress level is not repeatable, with values between sixty thousand and one million cycles, with no

discernible pattern as to cylindrical defects or double-conical defects. Thus it is hard to estimate the number of cycles to failure for the fatigue specimens at this stress level. When lowered to a 400 MPa stress level, the fatigue life of one specimen with a cylindrical defect was even twenty times more than two other specimens. When the maximum stress was lowered to 350 MPa, fatigue specimens with defects did not fail until after ten million cycles.

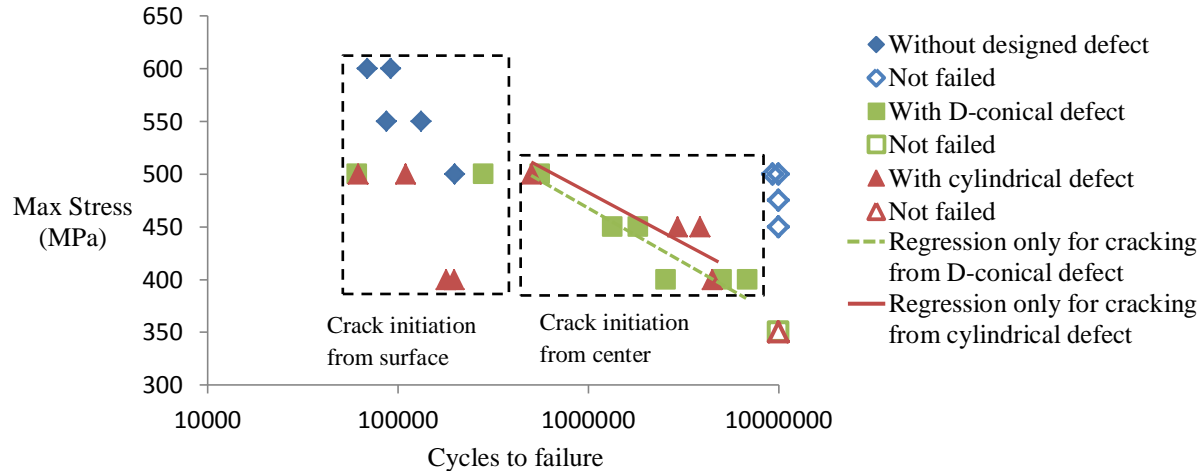


Fig. 4 Stress-life plot for fatigue testing of Ti64 specimens with and without geometric defects

Fractography

Generally the process of fatigue failure is characterized by crack initiation, crack propagation and final failure. Cracks usually initiate at the site with the highest stress concentration. A microscopic view of Ti64 fatigue specimens shows a series of radiating ridges on the fracture surface, which can be traced along the direction to identify the area of the fracture initiation. These radiating ridges occupy most of the fracture surface. In the final fast fracture area, “cup and cone” fracture is formed on the matching surfaces oriented at about 45 ° from the tensile axis.

For the fatigue specimens without designed defects, it was found that fatigue crack initiation only occurred at the surface. Fatigue fracture for some specimens occurred outside the gauge section and the fracture extended to the whole cross section and finally failed. Fig. 5 shows a typical fracture surface whose fatigue crack initiated at the gauge surface. A boundary deficiency can be seen at the crack initiation site. The crack propagated from the initiation site over several cycles. Final fracture occurred when the remaining area was too small to carry the maximum load of the final cycle. XRD analysis indicates as-built SLM Ti-6Al-4V contains an HCP phase with both α -phase and α' martensite [10, 11]. Therefore, the radiating ridges refer to transgranular cleavage of α and α' grains. The low failure cycles of these specimens can be attributed to crack growth from some of the α or α' grains with very little crack initiation time. Micro striations on grain surfaces can be observed in the crack propagation region at a higher magnification as shown in Fig. 5 (e) and (f). It is assumed that a transition from transgranular cleavage to classic fatigue striations occurred and then changed to final fast fracture in ductile dimple mode [12]. The orientation of these striations varied from grain to grain. Dimpled appearance which is characteristic of microvoid coalescence is exhibited in the final fast fracture area. Some regions are located between dimpled areas and appear to be smooth at low magnification.

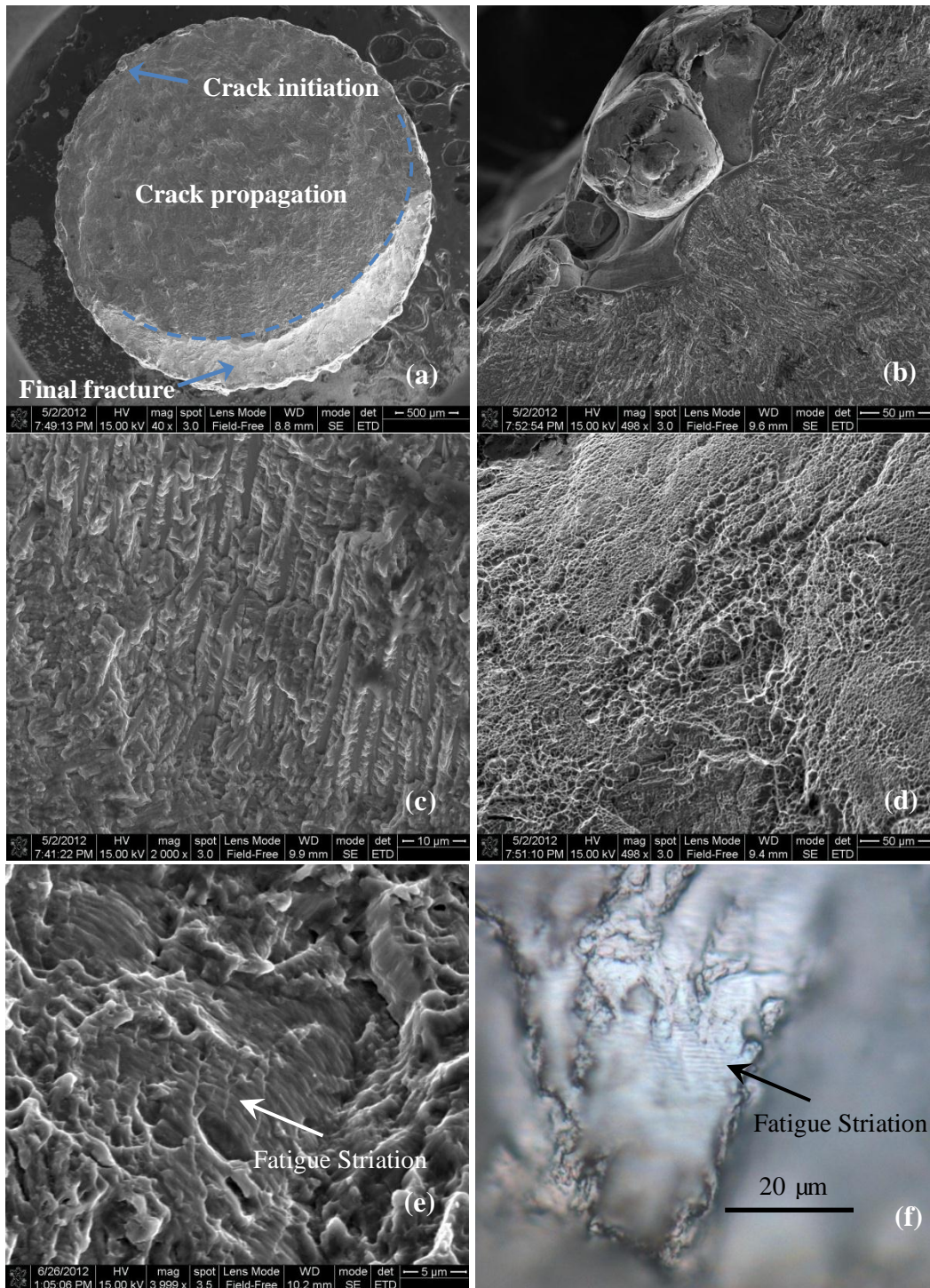


Fig.5. Fractography of fatigue specimen (crack initiated from gauge surface) (a) Top view, (b) Crack initiation site, (c) Crack propagation (transgranular fracture), (d) Final fast fracture region, (e) Fatigue striation in crack propagation region (SEM), (f) Fatigue striation (optical microscopy)

The fracture pattern of fatigue specimens with designed defects is varied, initiating either from the surface of the gauge section or from the designed defect in the interior. Thus, the stress-life plot can be divided into two areas for failed fatigue specimens as shown in Fig. 4. The former

fracture pattern has a similar fractography as shown in Fig. 5, accompanied with a lower fatigue life than the latter fracture pattern. This explains why there is such large scatters amongst the fatigue life data for certain stress levels.

When the fatigue crack was initiated from the designed cylindrical defect, the fracture surface is close to an edge of the defect, as shown in Fig. 6. The crack initiated from one of the defect's boundaries. This indicates that geometry-dependent stress concentrations at the edge of a defect can be the cause of crack initiation. However, it is difficult to identify the specific crack initiation site with respect to one of these the α or α' grain facets. The primary grains in the initiation site may all have orientation pointing along crack propagation. A transgranular cleavage took place in the crack propagation region from and around the crack initiation site, followed by ductile-dimple fast fracture.

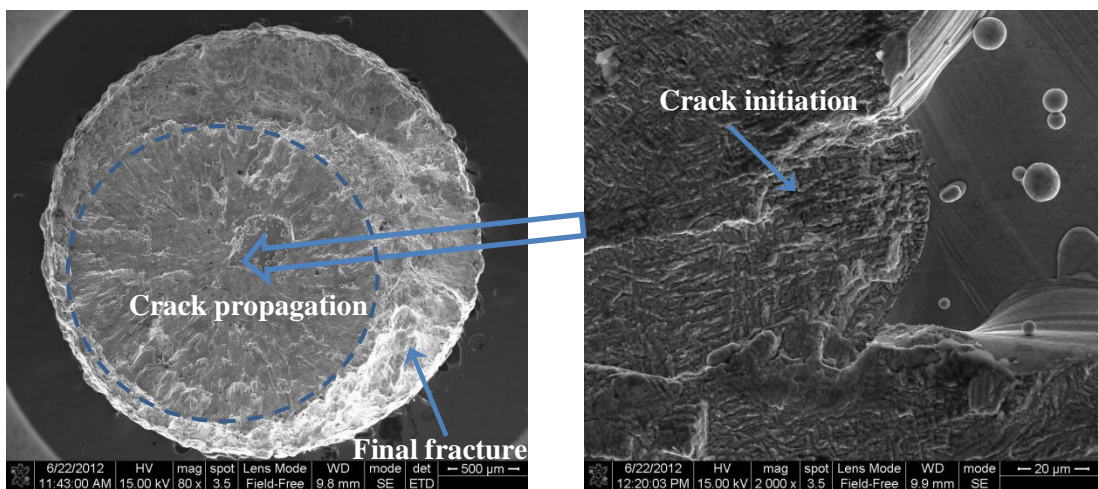


Fig. 6 Fracture surface of fatigue specimen (crack initiated from central cylindrical defect)

Fig. 7 shows a typical fracture surface with a crack initiated from the double-conical defect. Transgranular cleavage is the primary crack propagation pattern. Ductile dimple appearance is seen in the fast fracture region.

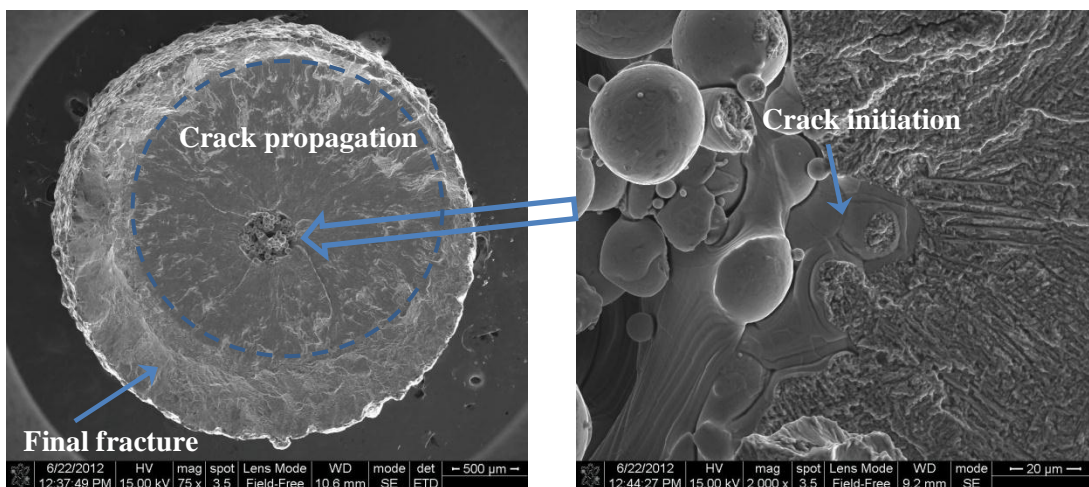


Fig. 7 Fracture surface of fatigue specimen (crack initiated from central double-conical defect)

According to the fundamentals of fracture mechanics, both cylindrical and double-conical defects should have a detrimental effect on the fracture strength because the applied stress will be amplified near the defect. The magnitude of this amplification depends on crack orientation and geometry. However, fractography shows no apparent difference in the fracturing process between cylindrical defects and double-conical defects. Moreover, the regression lines show similar tendency between these two types of defects as shown in Fig. 4, if only crack initiations from designed defect are considered in the regression. This indicates that these two defect morphologies do not result in apparent difference of stress amplification with respect to crack initiation.

The rough surface of the gauge section contains a random distribution of defects within the gauge surface. These defects negatively impact the fatigue life as stress risers and cause quick failure of Ti-6Al-4V fatigue specimens under the higher stress intensities. This is demonstrated from the stress-life plot in Fig. 4. It was found that as-built fatigue specimens are susceptible to fatigue crack initiation from the surface when the maximum stress is larger than 500 MPa. Fatigue specimens with designed defects should encounter the same situation, although no fatigue tests were conducted at stress levels above 500 MPa for those specimens. At stresses below 500MPa, as-built surface defects have no apparent impact on fatigue life. This could be the result of microstructural characteristics around surface defects compared to those near designed internal defects. When Ti-6Al-4V fatigue specimens are free from any internal/surface defects or the defects are not sufficient enough to act as stress raisers then the fatigue properties are strongly influenced by the morphology and arrangement of the α and β phases. SLM fabricated Ti-6Al-4V exhibits a lamellar microstructure. In lamellar microstructures fatigue cracks initiate at slips bands within α (α') lamellae or at α (α') along prior β grain boundaries [13]. This can result in crack initiation to occur from the interior. Thus, in addition to the role of defects themselves, further investigations are merited to better understand the microstructural differences between skin and core areas of SLM-produced Ti-6Al-4V specimens to help understand how these might affect crack initiation.

Conclusion

Defects play a critical role in SLM Ti-6Al-4V fatigue specimen performance. As-built surfaces become crack initiation sites, especially when the stress intensity is higher than 500 MPa. Designed internal defects also affect the fatigue life of SLM Ti-6Al-4V materials so that the fatigue limit is lowered during fatigue testing. In these tests, no significant differences between cylindrical and double-conical defects were observed. In order to explain the effect of defects on Ti-6Al-4V fatigue life, further studies concerning the microstructure and morphology of the surface of fatigue specimens are required.

Acknowledge

The authors gratefully acknowledge the support of the Office of Naval Research, awards N00014-09-1-0147 and N00014-10-1-0800, Technical Monitor: Dr. Ignacio Perez. The authors also express their gratitude to the staff of the Rapid Prototyping Center at the University of Louisville for their assistance.

Reference

- [1] American Society for Testing and Materials (ASTM). Standard Terminology for Additive Manufacturing Technologies (F2792-12). <http://www.astm.org>.
- [2] I. Gibson, D.W. Rosen, B. Stucker. Additive Manufacturing Technologies: Rapid Prototyping to Direct Digital Manufacturing. Springer, New York, NY, 2009
- [3] G. Levy, R. Schindel, J.P. Kruth. Rapid manufacturing and rapid tooling with layer manufacturing (LM) technologies, state of the art and future perspectives. *CIRP Annals-Manufacturing Technology*, 52(2), 2003, 589-609
- [4] B. Vandenbroucke, J.P. Kruth. Selective laser melting of biocompatible metals for rapid manufacturing of medical parts. *Rapid Prototyping Journal*, 13(4), 2007, 196-203
- [5] W.O. Soboyejo, T.S. Srivatsan. Advanced Structural Materials: Properties, Design Optimization, and Applications. CRC Press 2006, 359-400
- [6] S. Kumar. Microstructure and Wear of SLM Materials. *Solid Freeform Fabrication Symposium*, 2008, 128-142
- [7] M.K.E. Ramosoou, G. Booyesen, T.N. Ngonda, et al. Mechanical Properties of Direct Laser Sintered Ti-6Al-4V. *Materials Science and Technology Conference (MS&T)*, 2011, 1460-1468
- [8] B. Van Hooreweder, D. Moens, R. Boonen, et al. Analysis of fracture toughness and crack propagation of Ti6Al4V produced by selective laser melting. *Advanced Engineering Materials*, 14(1-2), 2012, 92-97
- [9] EOS Titanium Ti64-for aerospace and engineering applications and biom. EOS GmbH (www.eos.info)
- [10] L. Facchini, E. Magalini, P. Robotti, et al. Ductility of a Ti-6Al-4V alloy produced by selective laser melting of prealloyed powders. *Rapid Prototyping Journal*, 16(6), 2010, 450-459
- [11] L.E. Murr, S.M. Gaytan, D.A. Ramirez, et al. Metal Fabrication by Additive Manufacturing Using Laser and Electron Beam Melting Technologies. *J. Mater. Sci. Technol.*, 28(1), 2012, 1-14
- [12] W.A. Glaeser, B.H. Lawless. Behavior of alloy Ti-6Al-4V under pre-fretting and subsequent fatigue conditions. *Wear*, 250, 2001, 621-630
- [13] T. Mohandas, D. Banerjee, V.V. Kutumba Rao. Fusion zone microstructure and porosity in electron beam welds of an $\alpha+\beta$ titanium alloy. *Metal. Trans.* 30A, 1998, 789-798